



OPEN

Reduced microbial diversity of the nasopharyngeal microbiome in household contacts with latent tuberculosis infection

Cinthya Ruiz-Tagle¹, Juan A. Ugalde², Rodrigo Naves³, Rafael Araos^{4,5}, Patricia García⁶ & María Elvira Balcells¹✉

The upper respiratory tract is an obliged pathway for respiratory pathogens and a healthy microbiota may support the host's mucosal immunity preventing infection. We analyzed the nasopharyngeal microbiome in tuberculosis household contacts (HHCs) and its association with latent tuberculosis infection (TBI). A prospective cohort of HHCs was established and latent TBI status was assessed by serial interferon- γ release assay (IGRA). Nasopharyngeal swabs collected at baseline were processed for 16S rRNA gene sequencing. The 82 participants included in the analysis were classified as: (a) non-TBI [IGRA negative at baseline and follow-up, no active TB (n = 31)], (b) pre-TBI [IGRA negative at baseline but converted to IGRA positive or developed active TB at follow-up (n = 16)], and (c) TBI [IGRA positive at enrollment (n = 35)]. Predominant phyla were *Actinobacteriota*, *Proteobacteria*, *Firmicutes* and *Bacteroidota*. TBI group had a lower alpha diversity compared to non-TBI ($p_{\text{adj}} = 0.04$) and pre-TBI ($p_{\text{adj}} = 0.04$). Only TBI and non-TBI had beta diversity differences ($p_{\text{adj}} = 0.035$). Core microbiomes' had unique genera, and genus showed differential abundance among groups. HHCs with established latent TBI showed reduced nasopharyngeal microbial diversity with distinctive taxonomic composition. Whether a pre-existing microbiome feature favors, are a consequence, or protects against *Mycobacterium tuberculosis* needs further investigation.

Tuberculosis (TB) is an airborne infectious disease caused by the pathogenic bacteria *Mycobacterium tuberculosis* (Mtb). About a quarter of the global population is infected with Mtb¹. The susceptibility to acquiring this infection depends on intensity² and duration of exposure³. Host characteristics such as sex, age, genetics, immune status, nutrition, and environmental and social factors (crowding, poor ventilation, alcohol, smoking, and occupational risk) increase the risk of TB^{4,5}; still, individuals with no known risk factors account for a large number of new cases.

The microbiota inhabiting our body provides a milieu that benefits the entire host-microbe system, influencing host homeostasis and immune response^{6,7}, with each person having distinct microbe communities. A healthy microbiota supports the host's immunity against infections by promoting mucosal barrier function, competing with pathogens, and priming immune responses. At the same time, its disruption can increase the risk of disease^{8,9}. The upper respiratory tract is colonized by specialized resident bacterial assemblages, presumably preventing potential pathogens from overgrowing and disseminating toward the lungs, thereby functioning as gatekeepers to respiratory health¹⁰. The characteristics of the nasal and nasopharyngeal microbiome from infected and uninfected individuals have been shown to differ in upper respiratory tract infections such as sinusitis, otitis media, influenza, RSV, and SARS-CoV-2^{11,12}.

There is less evidence about the nasopharyngeal microbiota composition in lower respiratory tract bacterial infections. Two studies reported comparatively lower alpha diversity indices of microbial diversity in children with pneumonia^{13,14}, while another study in adults did not. Nonetheless, the three studies reported that a more

¹Departamento de Enfermedades Infecciosas del Adulto, Escuela de Medicina, Pontificia Universidad Católica de Chile, Santiago, Chile. ²Center for Bioinformatics and Integrative Biology, Facultad de Ciencias de La Vida, Universidad Andrés Bello, Republica 330, Santiago, Chile. ³Instituto de Ciencias Biomédicas, Facultad de Medicina, Universidad de Chile, Santiago, Chile. ⁴Instituto de Ciencias E Innovación en Medicina, Facultad de Medicina Clínica Alemana, Universidad del Desarrollo, Santiago, Chile. ⁵Advanced Center for Chronic Diseases (ACCDiS), Santiago, Chile. ⁶Laboratorio de Microbiología, Departamento de Laboratorios Clínicos, Escuela de Medicina, Pontificia Universidad Católica de Chile, Santiago, Chile. ✉email: ebalcells@uc.cl

diverse microbiota is found in the nasopharynx of healthy individuals^{13–15}. In addition, the experimental nasal inoculation of *Streptococcus pneumoniae* was shown to induce a shift in the nasopharyngeal microbiota of healthy adults correlating with the establishment of the bacterial carriage¹⁶.

In TB pathogenesis, the role of the respiratory tract microbiome remains largely unexplored. Thus, we assessed the nasopharyngeal microbiome in a prospective cohort of individuals exposed to Mtb to ascertain if there are differences in microbiome composition or abundance between individuals that acquired or not a latent TB infection, aiming to gain further insight into TB pathogenesis and susceptibility.

Results

Clinical and demographic data. From the enrolled cohort of 231 HHCs, 155 participants (67%) had complete follow-up and fulfilled inclusion/exclusion criteria for microbiome analysis (Supplementary Fig. S1). As per our classification, 44% were classified as TBI (n=69), 41% as non-TBI (n=63), and 15% as pre-TBI (n=23).

From the 155 samples selected for 16S sequencing, 82 (53%) remained after the ASVs filtering process, with a considerable loss due to the initial low microbial biomass of the nasopharyngeal swabs collected samples. For analysis, 31 (38%) samples pertained to the Mtb uninfected (non-TBI), 16 (19%) from those acquiring a new Mtb infection on follow-up (pre-TBI), and 35 (43%) from HHCs displaying Mtb infection since the baseline evaluation (TBI). The demographic and clinical characteristics of HHCs included in the analysis are summarized in Table 1. Overall, 58.5% were female, the mean age was 34.5 (\pm 13.7) years, and all were residents in Chile of Hispanic/Latino descent, primarily migrants from Peru (58.5%). Individuals with TBI were slightly older than non-TBI and pre-TBI (p=0.013). The comparison of the demographic and clinical characteristics of the entire cohort (composed of individuals whose samples were excluded, unsuccessfully sequenced, and successfully sequenced/analyzed) did not reveal substantial differences between groups and is summarized in Supplementary Table S1.

Bacterial relative abundance in the nasopharynx of HHCs. After dataset cleaning and filtering, 841 ASVs remained for evaluation. A descriptive analysis of relative abundance showed that for all HHCs, a total of 14 phyla were found, with the most predominant being: *Actinobacteriota* (43.8%), *Proteobacteria* (31.2%), *Firmicutes* (19.6%), and *Bacteroidota* (2.5%) (Table 2). There was variability in the predominance of less abundant phylum within each group (Supplementary Table S2) and a high degree of individual variability within groups (Fig. 1a). At the class level, for all HHCs, a total of 19 bacterial classes were found, dominating *Actinobacteria* (43.4%), *Alphaproteobacteria* (15.7%), *Gammaproteobacteria* (15.6%) and *Bacilli* (13.7%) (Table 3). Class domination varied for less abundant classes within each group (Supplementary Table S3) and a high individual variability within groups was also observed (Fig. 1b). At the genus level, the most frequently found were *Corynebacterium* (25%), *Cutibacterium* (7%), *Lawsonella* (6.9%), *Dolosigranulum* (6.1%), *Paracoccus* (5.7%) and *Staphylococcus* (5.5%). Groups exhibited a high degree of individual variability within each one (Fig. 1c). The *Mycobacterium* genus was not detected by 16S analysis in any of the analyzed participants, nor the bacteria itself by culture of the contralateral nasopharyngeal swabs.

In addition, we also compared the relative abundance of the ASVs classified at the species level. Although the length of the analyzed region is too short to distinguish among all present microbial species, some unique matches based on the region analyzed can be distinguished (Supplementary Fig. S2). Among the taxa present, there are some taxa prevalent in a large fraction of the samples in all groups, such as *Cutibacterium granulosum* (6.1%). Some species were more prevalent (present in at least 50% of the samples) in some of the groups. For example, *Dolosigranulum pigrum* (7.5%) was present in more than 50% of the samples of the non-TBI group.

	Non-TBI (n = 31)	Pre-TBI (n = 16*)	TBI (n = 35†)	p-value
Female sex (n, %)	16 (51.6%)	10 (62.5%)	22 (62.9%)	0.611
Mean age, years (SD)	32.5 (11.8)	27.9 (12.0)	39.2 (14.7)	0.013
Countries, total (n, %)				0.222
Peru	17 (54.8%)	9 (56.3%)	22 (62.9%)	
Chile	9 (29.0%)	1 (6.3%)	8 (22.9%)	
Other Latin American countries	5 (16.1%)	6 (37.5%)	5 (14.3%)	
Tobacco smoker (n, %)	8 (25.8%)	3 (18.8%)	10 (28.6%)	0.683
Self-reported viral respiratory infections in last month (n, %)	10 (32.3%)	5 (31.3%)	13 (37.1%)	0.883
Any antibiotic use—Last 6 months (n, %)	7 (22.6%)	1 (6.3%)	5 (14.3%)	0.386
Probiotic or vitamin use—Last 3 months (n, %)	7 (22.6%)	3 (18.8%)	2 (5.7%)	0.125
Proton pump inhibitor or antacids—Last 3 months (n, %)	4 (12.9%)	0 (0.0%)	9 (25.7%)	0.058
Vegan or Vegetarian diet	1 (3.2%)	0 (0%)	0 (0%)	0.573

Table 1. Clinical and epidemiological characterization of TB contacts included in the analysis (n = 82). * n = 3 individuals (18.8%) developed active TB at follow-up. † n = 2 individuals (5.7%) developed active TB at follow-up. Statistical analysis were performed with analysis of variance (ANOVA) for continuous variables, and Fisher's exact or Chi-squared test for categorical variables. Statistical significance was considered when p-values < 0.05 (two-tailed).

Phylum	Average (%)	Standard deviation (%)
Actinobacteriota	43.820	23.256
Proteobacteria	31.242	20.099
Firmicutes	19.557	17.273
Bacteroidota	2.530	5.351
Cyanobacteria	1.014	1.402
Patescibacteria	0.753	1.092
Fusobacteriota	0.348	1.173
Chloroflexi	0.257	0.686
Deinococcota	0.206	0.557
Planctomycetota	0.168	0.664
Acidobacteriota	0.082	0.198
Armatimonadota	0.025	0.140

Table 2. Percentage distribution at phylum level for all nasopharyngeal samples analyzed after amplicon sequence variant filtering (n = 82).

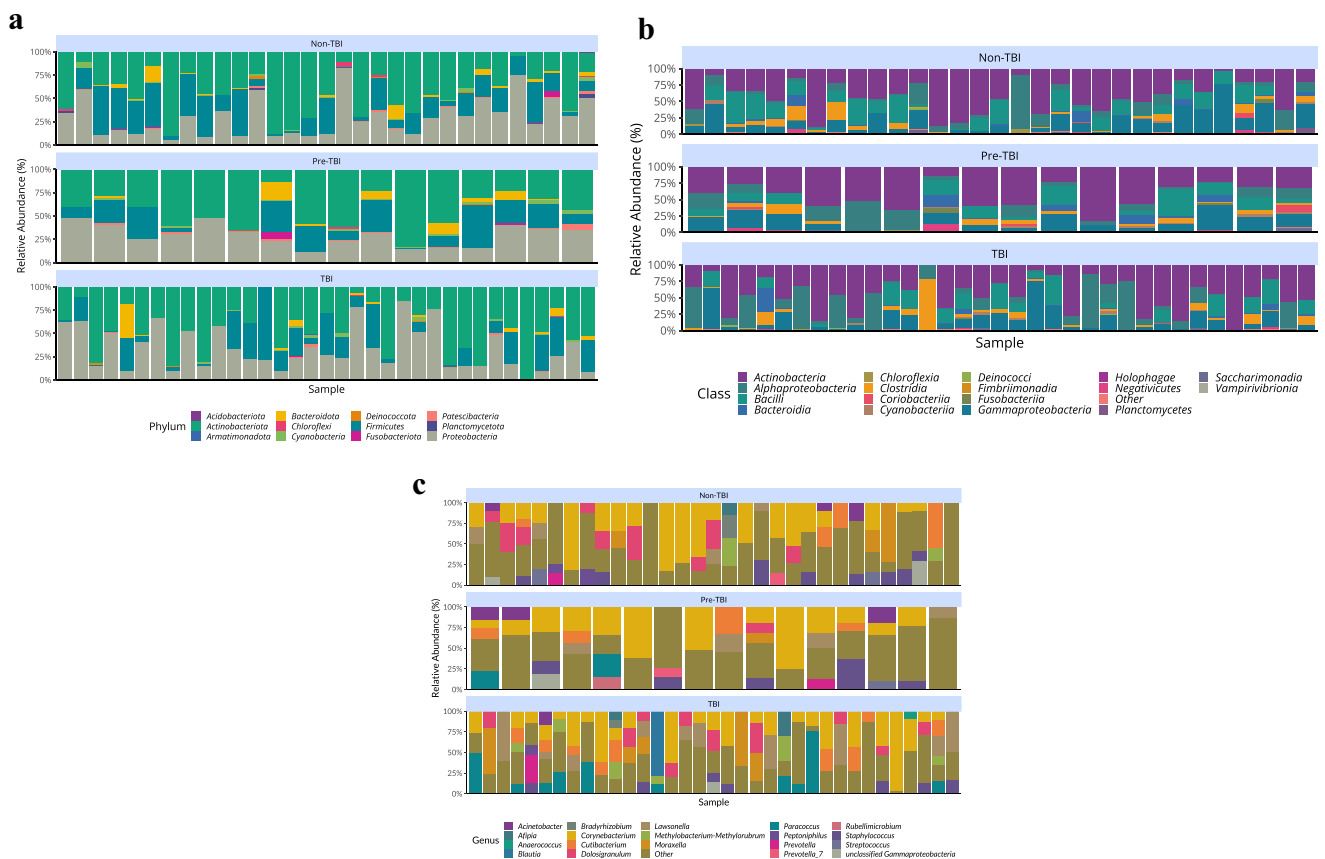


Figure 1. Taxonomic classification of the nasopharynx microbiota in TB exposed household contacts (n = 82). Descriptive individual variability of relative abundance according to LTBI uninfected (non-TBI), new LTBI on follow-up (pre-TBI) and LTBI from baseline evaluation (TBI) groups at (a) Phylum, (b) Class and (c) Genus level.

In contrast, *Kocuria rosea* (1.1%) was found in more than 50% of the samples of the TBI group (Supplementary Fig. S3).

Bacterial diversity in the nasopharynx of HHCs. *Alpha diversity.* Community diversity composition between HHCs groups was compared using the Shannon diversity index. The comparison showed significant differences between the group medians (non-TBI: 3.23 [2.76–3.75]; pre-TBI: 3.29 [2.87–3.97]; TBI: 2.64 [2.05–3.26], $p = 0.01$). Posthoc analysis using the Wilcoxon test showed statistical differences between the non-TBI vs. TBI group ($p_{\text{adj}} = 0.04$) and the pre-TBI vs. TBI group ($p_{\text{adj}} = 0.04$) (Fig. 2a). These results indicate that the

Class	Average (%)	Standard deviation (%)
Actinobacteria	43.402	23.343
Alphaproteobacteria	15.651	19.288
Gammaproteobacteria	15.590	15.856
Bacilli	13.701	13.554
Clostridia	5.253	9.608
Bacteroidia	2.530	5.351
Cyanobacteriia	0.969	1.363
Saccharimonadia	0.753	1.092
Negativicutes	0.603	1.573
Coriobacteriia	0.394	1.471
Fusobacteriia	0.348	1.173
Chloroflexia	0.257	0.686
Deinococci	0.206	0.557
Planctomycetes	0.168	0.664
Holophagae	0.082	0.198
Vampirivibrionia	0.044	0.196
Fimbriimonadia	0.025	0.140
Acidimicrobiia	0.023	0.097

Table 3. Percentage distribution at class level for all nasopharyngeal samples analyzed after amplicon sequence variant filtering (n = 82).

microbiome of the participants with a latent TB infection had lower alpha diversity than the non-infected, including those non-infected but subsequently acquiring Mtb on follow-up, suggesting that structural differences may arise after acquiring Mtb.

Beta diversity. The microbial community composition comparison showed significant differences between groups ($p = 0.036$) (Fig. 2b) that the dispersion of the centroids could not explain within the dataset ($p = 0.233$). Pairwise comparison indicated only the communities between the non-TBI and the TBI group were different ($p_{\text{adj}} = 0.035$), while those of pre-TBI and TBI ($p_{\text{adj}} = 0.095$) and non-TBI and pre-TBI ($p_{\text{adj}} = 0.189$) were not. Thus, infected and uninfected individuals showed differences in the beta diversity of microbial communities, but the smaller group of those who later acquired the infection did not.

Core microbiome. Evaluation of the core microbiome was performed for each HHCs group separately. At the ASV level, only a few ASVs were present in at least 50% of all samples from each group (non-TBI, 12 ASVs; pre-TBI, 6 ASVs; TBI, 2 ASVs). TBI and non-TBI, as well as TBI and pre-TBI, did not share any common ASVs. However, pre-TBI and non-TBI shared five ASVs (*Methylobacterium-Methylorubrum*, *Afipia*, *Bradyrhizobium*, *Leptolyngbya* PCC-6306, and *Kocuria rosea*), and TBI, pre-TBI and non-TBI shared only one (*Cutibacterium granulosum*) (Fig. 3a). Among unique ASVs in each group, six were associated with the non-TBI group (*Dolosigranulum pigrum*, *Mesorhizobium*, *Cupriavidus necator*, *Variovorax*, *Lawsonella* and *Microbacterium*), and 1 with the TBI group (*Paracoccus*).

At the genus level, we identified a core set of genera present in at least 50% of all samples within each group (non-TBI, 25; pre-TBI, 20; TBI, 13). There were 13 genera shared between the three of them (*Acinetobacter*, *Afipia*, *Bradyrhizobium*, *Corynebacterium*, *Cupriavidus*, *Cutibacterium*, *Kocuria*, *Lawsonella*, *Methylobacterium-Methylorubrum*, *Paracoccus*, *Pseudomonas*, *Staphylococcus* and *Streptococcus*), five between non-TBI and pre-TBI (*Clostridium sensu stricto* 1, *Legionella*, *Undibacterium*, *Leptolyngbya* PCC-6306, and TM7a), and none between pre-TBI and TBI, and non-TBI and TBI. Additionally, the non-TBI group had seven unique genera (*Finegoldia*, *Romboutsia*, *Dolosigranulum*, *Mesrhizobium*, *Rickettsiella*, *Variovorax* and *Microbacterium*). In contrast, the pre-TBI had only two (*Sphingomonas* and *Rothia*), and the TBI had none (Fig. 3b).

Differentially abundant genera between HHC groups. We used compositional-based analysis to evaluate differentially abundant genera between the three HHCs groups. Statistically significant differences (log fold changes) were found for non-TBI compared to pre-TBI, with *Reyranella* and *Micrococcus* being more abundant in the non-TBI group. At the same time, *Megasphaera* and *Burkholderia-Caballeronia-Paraburkholderia* were more abundant in the pre-TBI group (Fig. 4a). In addition, for non-TBI vs. TBI, *Leptotrichia* and *Afipia* were more abundant in the non-TBI group (Fig. 4b). For pre-TBI vs. TBI, seven genera, *Reyranella*, *Polaromonas*, *Nocardiodetes*, *Micromonospora*, *Micrococcus*, *Deinococcus*, and *Acidivorax*, were more abundant in the TBI group (Fig. 4c). Finally, *Reyranella* was consistently lower in the pre-TBI dataset.

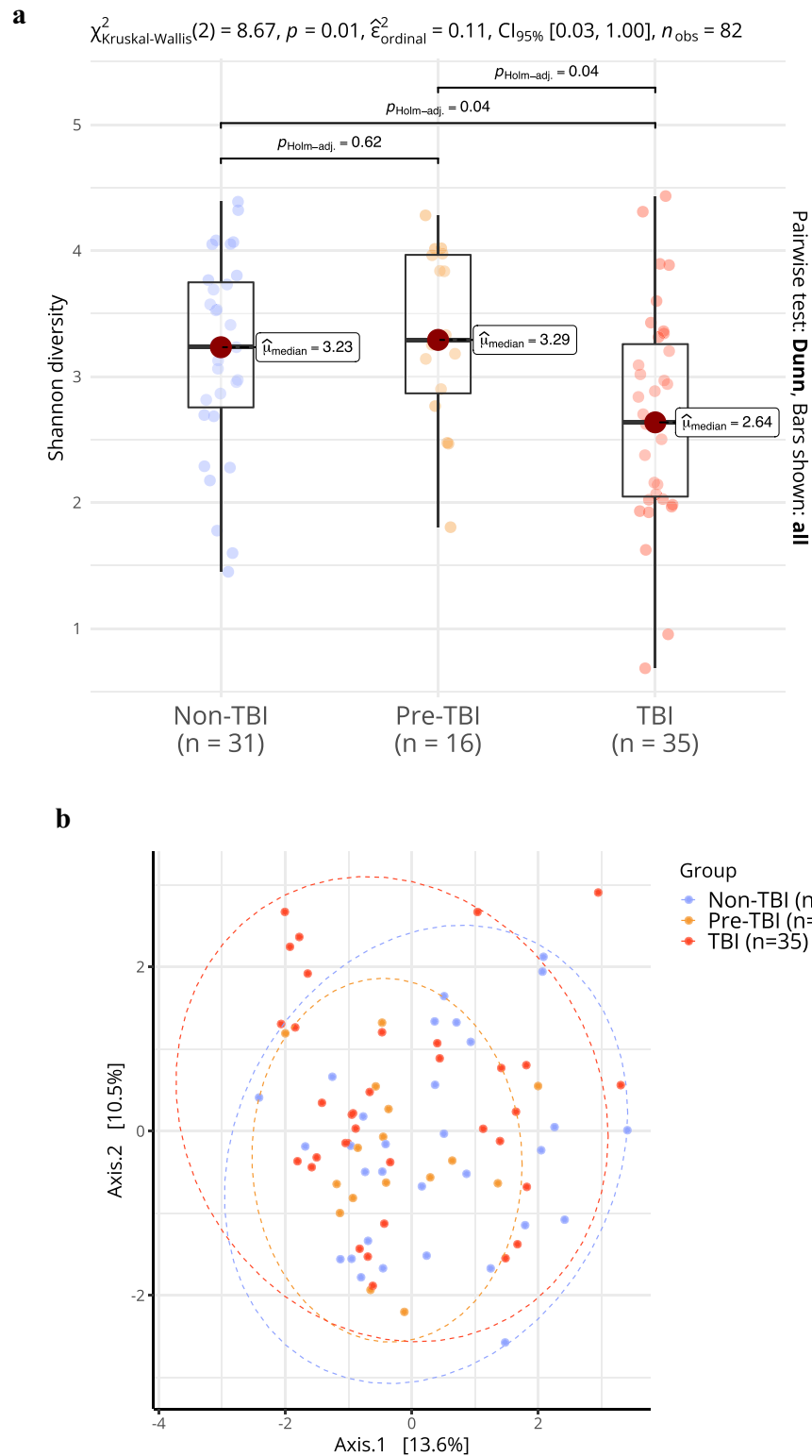


Figure 2. Changes in microbial diversity in the nasopharynx microbiota in TB exposed household contacts (n = 82). **(a)** Alpha diversity in HHCs samples using Shannon index. **(b)** Principal Coordinate Analysis plot showing the Euclidian distance of the PhiR-transformed data for each of the samples. Differences between group composition were significant (p = 0.036), only the comparison between non-TBI versus TBI (p = 0.035). Statistical analysis for alpha diversity was performed with Kruskal–Wallis test followed by Wilcoxon test with Holm adjustment for multiple testing. For beta diversity, a permutational analysis of variance based on the Euclidean distance matrix was performed.

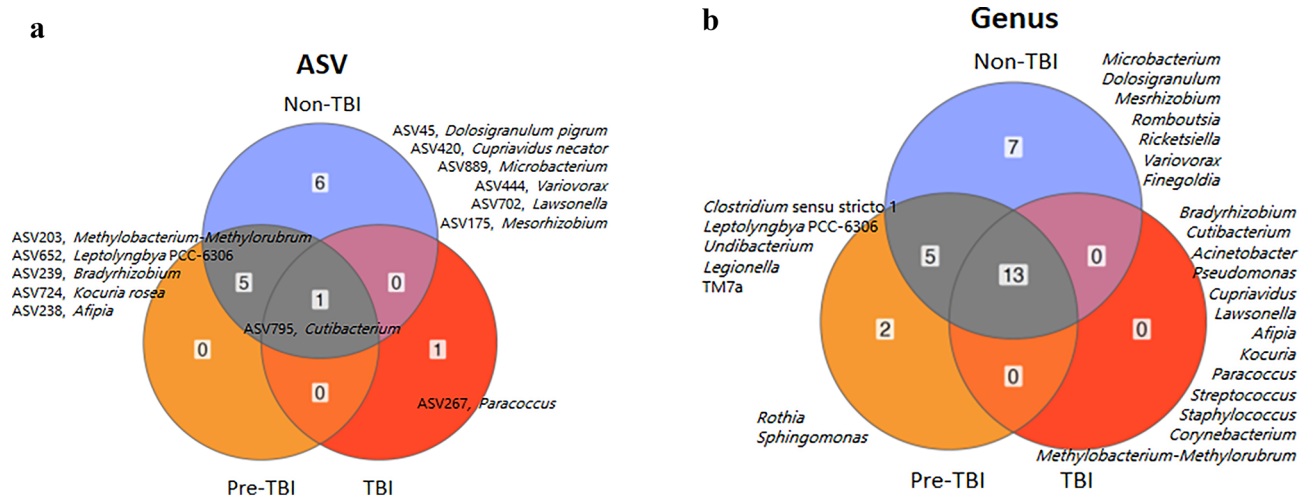


Figure 3. Core microbiome by TB infection status group, showing in each case ASVs or Genus that are present in at least 50% of the individuals within that group. (a) ASVs unique and shared among all groups. Names indicated the ASV number and its best taxonomic classification up to the species level. (b) Genus that are unique and shared between all groups. To identify taxonomic groups with statistically significant differences in abundance between groups was performed with the compositional approach implemented in ANCOMBC.

Discussion

In the present study, we assessed the nasopharyngeal microbiome of a population of HHCs of patients with active TB. We found that individuals with an acquired latent TBI had a lower alpha diversity than uninfected individuals. Our results are consistent with reports of both nasal and oropharynx samples of patients with active PTB disease, who had a less diverse microbiota compared to healthy controls¹⁷, as well as the analysis of gut microbiota of children with PTB that reported a decreased microbial diversity¹⁸. Nonetheless, the findings observed in microbiota diversity in contacts who were about to acquire the infection remain to be confirmed in a larger cohort. Previous work by our group and others has reported that transient Mtb localization in the upper respiratory tract mucosa can rarely occur after exposure to a PTB case^{19,20}. However, the persistence, replication and direct effect of Mtb in nasopharyngeal mucosa is unlikely, as we did not detect Mtb in the nasopharyngeal samples.

The interaction between intestinal microbial communities and the resident immune cells in the mucosa can lead to modulation of local and systemic immune response; an increased susceptibility to specific respiratory diseases (the “gut–lung axis”) has been proposed to develop when microbial dysbiosis occurs²¹. In murine models, broad-spectrum antibiotics-driven changes in the gut microbial composition affect the survival, burden, and dissemination of Mtb in the lungs, liver, and spleen compared to the mice with intact microbiota. Furthermore, fecal transplantation succeeds in restraining Mtb growth in the lungs preventing its dissemination²². Of interest, both macaques challenged with Mtb and household contacts having a latent TBI are less likely to progress to active TB when infected with *Helicobacter pylori*²³. Although less explored, the upper and lower respiratory tract may also display immune system/microbiota interactions. In mice models, nasal instillation of *Staphylococcus aureus* attenuates influenza-mediated lethal inflammation in the lungs by inducing M2 alveolar macrophages²⁴, and *Lactobacillus plantarum* administration protects against lethal pneumovirus infection in the lungs by TLR2 and NOD2 receptor signaling²⁵.

The present study’s overall analysis of nasopharyngeal microbiota showed that for all HHCs, the predominant phyla were *Actinobacteriota*, *Proteobacteria*, *Firmicutes* and *Bacteroidota*. These results are consistent with other reports of the nasopharyngeal microbiota, with variations in their relative abundances^{17,26–31}, and with microbiome studies of nasal and oropharynx samples from patients with active TB compared to uninfected individuals¹⁷. Interestingly, HHCs not acquiring latent TBI had a higher relative abundance mean (above 5%) of *Corynebacterium*, *Dolosigranulum*, *Cutibacterium* and *Staphylococcus*, similar to what is found in healthy non-exposed individuals³², while HHCs with an establish LTBI or those about to acquire a latent TBI had a higher relative abundance of *Corynebacterium*, *Lawsonella*, *Paracoccus*, *Cutibacterium*, *Dolosigranulum*, *Moraxella*, and *Corynebacterium*, *Staphylococcus*, *Cutibacterium*, *Lawsonella* and *Paracoccus*, respectively.

Our study is among the few that have analyzed the human nasopharyngeal microbiome in the latent TBI³³ and, to our knowledge, the first to examine highly exposed HHCs from a prospective cohort acquiring or not Mtb infection at follow-up. However, there are several reports about gut^{34,35} and lungs’ microbiome characteristics of patients with established active PTB^{17,36–39}, recurrent TB, and TB treatment failure⁴⁰, with most studies including patients undergoing antimicrobial therapy. Regarding latent TBI, our findings differ from those of a study involving a comparatively small cohort size, in which the nasopharyngeal community diversity and microbial community composition of healthy controls (n = 18) were similar to that of latent TBI individuals (n = 19)³³. These dissimilarities could lie in our control group that despite not having acquired the infection had being highly exposed to Mtb. Also, the differences could arise in the smaller number of patients included in that report and in the analytic approach, as the authors sequenced the V3-V4 region of the 16S rRNA gene and evaluated microbial diversity by looking at operational taxonomic units (OTUs) with a 97% or higher level of

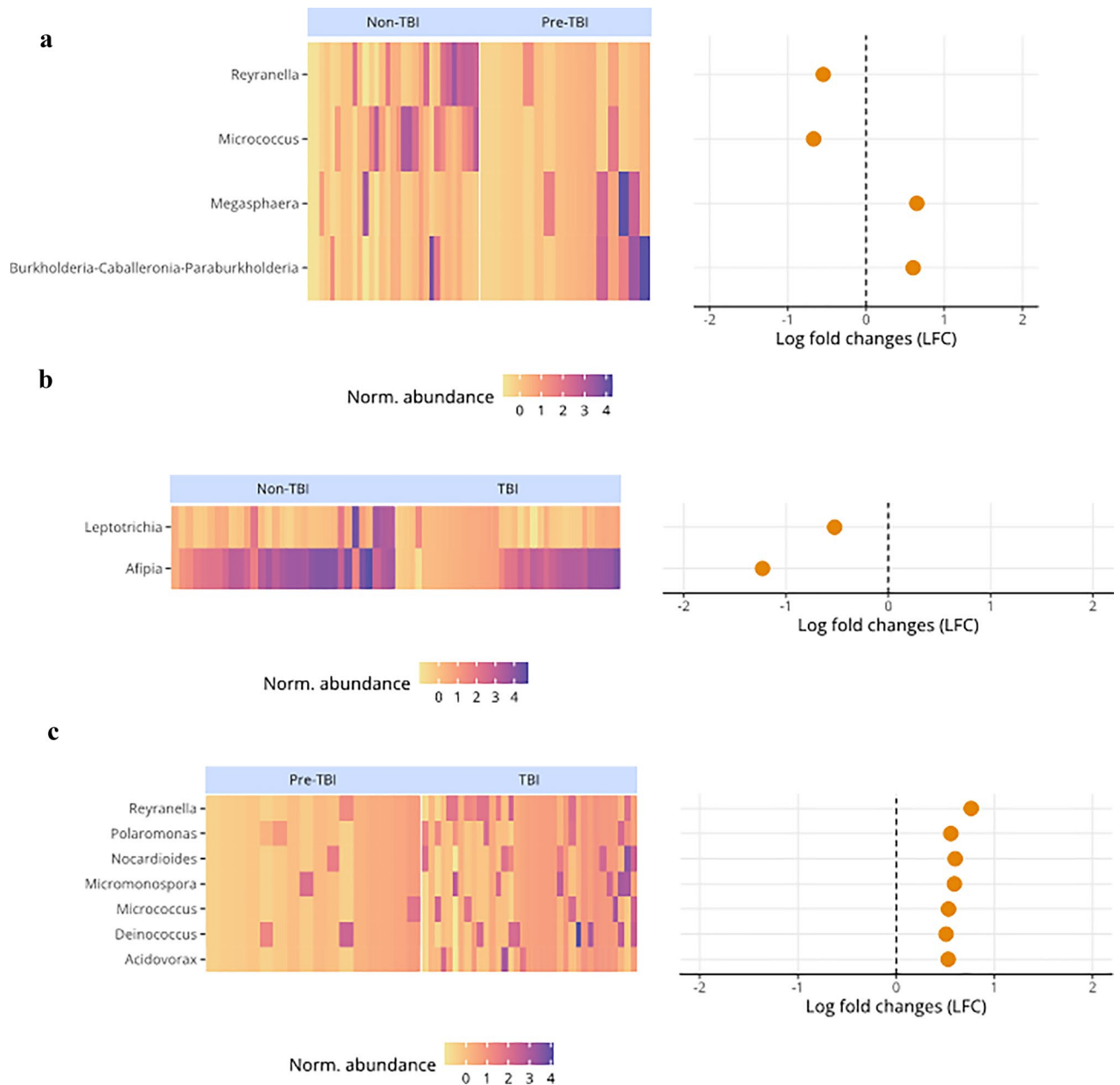


Figure 4. Genera with statistically significant differential abundance comparing household contacts ($n = 82$) TB infection status. (a) non-TBI vs. pre-TBI, (b) non-TBI vs. TBI, and (c) pre-TBI vs. TBI.

sequence similarity. In the current study, we sequenced the V1-V3 region which allows better resolution (even at the species level) for samples from human oral and respiratory tracts⁴¹, and also used ASVs, which allows for improved discrimination of ecological patterns⁴². Although not the scope of our study, the same authors found differences at the phylum and class levels between active TB and latent TBI, but not in alpha nor in beta diversity.

The lung microbiome resembles the healthy upper respiratory tract microbiome¹⁰, and whether a healthy microbiota in the nasopharynx can prevent *Mtb* establishment in the lower respiratory tract epithelium is unknown. Our study does not support this, as we did not find significant differences in microbiome composition (beta diversity) and relative abundance between HHCs acquiring a new *Mtb* infection at follow-up from those who remained uninfected. Notwithstanding, the core microbiome showed that the genus *Dolosigranulum* was one among which detection was only in the uninfected individuals. *Dolosigranulum* and its combination with *Corynebacterium* are a potential keystone species in the upper respiratory tract microbiota. Reports have shown an association with nasal health in chronic rhinosinusitis⁴³, as well as a protective role in vitro experiments against *Staphylococcus aureus*⁴³ and *S. pneumoniae* colonization and otitis media in children^{44,45}. This protective effect might be mediated by *Dolosigranulum*'s antimicrobial properties (anti-inflammatory and barrier-enhancing) by exploiting TLR2/6 interaction mechanisms within the host cells and L-lactic acid production⁴³ or by its capacity to produce antibiotics or bioactive molecules that may play key roles in interspecies interactions

with its microbial neighbors, e.g., for niche competition⁴⁶. Both species are part of the healthy nasopharyngeal microbiota, even though *Dolosigranulum* has been rarely isolated from patients with bacteremia and queratitis⁴⁷. Nonetheless, carriage surveys focused on detection of *S. pneumoniae* indicates the nasopharynx as the natural habitat of this bacterium⁴⁷. Additionally, *Variovax*, also present only in non-infected HHCs, is a member of the human oral flora, has been previously identified as exclusive in nasal/oropharyngeal swabs of healthy participants compared to COVID-19 patients⁴⁸, and it is also known for its strong biofilm formation⁴⁹.

In our study, uninfected individuals who later acquired Mtb infection had a core microbiome that included the genus *Rothia*. Evidence shows that enrichment of lung microbiota with oral taxa such as *Rothia* induces host cellular mucosal immunity of the Th17/neutrophilic phenotype while suppressing innate immunity. Moreover, dysbiosis can predispose to or exacerbate conditions locally and at distal body sites⁵⁰. We also found that individuals who later acquired Mtb showed an enrichment of the opportunistic pathogen *Megasphaera*, which has also been reported to be more abundant in the oropharyngeal microbiota of individuals with viral pulmonary infections as in COVID-19⁵¹. Taken together, we may speculate that the lack of *Dolosigranulum*, together with the presence *Rothia* and *Megasphaera* reflect a dysbiosis that might have rendered individuals more susceptible to Mtb infection.

The core's microbiome present in at least 50% of Mtb infected individuals was represented only by *Paracoccus*, a gram-negative non-motile which genus, previously associated with infections, including leprosy and other skin infections where the skin microbiota had a relatively higher abundance of the bacteria compared to healthy controls^{52,53}.

Among the present study limitations were the loss of samples due to low biomass recovery in the nasopharyngeal sampling process, leading to low DNA sequencing quality. Additionally, we found mild differences in participant's age that may have partially contributed to the observed differences between groups. Although, this does not seem to be clinically relevant as our participants were young (median age 34.5) and alterations in nasal microbiota communities start in middle-aged adults (40–65 years)⁵⁴, similar to what has been found for gut microbiome that is relative stable in adults⁵⁵. A further limitation of the study is that despite being embedded in a prospective cohort, the microbiome analysis was done only at the baseline visit (cross-sectional sampling), so spurious ecological associations cannot be ruled out. The study of samples at follow-up visits would have allowed assessment of changes in microbiome composition before and after Mtb acquisition as well as assessing whether it is the LTBI that induces changes in the microbiota composition or conversely, whether the upper respiratory tract microbiota structure confers susceptibility to acquiring this infection.

In conclusion, our study shows that HHCs with established latent TBI have differences in the nasopharyngeal microbiome with reduced alpha diversity and different bacterial communities compared to uninfected individuals. Whether an immune modulation of all respiratory microbiota ensuing Mtb infection occurs, as it has been described for active TB disease, remains to be established, as well as the protective role it might grant.

Methods

Patient selection. A prospective cohort study of household contacts (HHCs) of active pulmonary TB (PTB) cases (only acid-fast smear-positive index cases), aged 15 years or older (n = 231), was conducted between September 2017 and February 2020 in Santiago, Chile⁵⁶. Contacts found to have active TB at baseline, reporting prior TB, autoimmune diseases, pregnancy, HIV infection, use of immunosuppressants, or inhalation drugs were not invited to participate. All HHCs were recruited within the first month after the TB diagnosis of the index case and screened for symptoms. Two nasopharyngeal swabs (one for 16S rRNA gene-targeted sequencing and another for Mtb culture) were taken at the baseline evaluation. Additionally, a chest X-ray to exclude secondary TB cases and an interferon- γ release assay (IGRA) test (QuantiFERON®-TB Gold Plus (QFT), QIAGEN, Hilden, Germany) were done at enrollment to evaluate TB infection (TBI) status. IGRA testing was repeated at a 12-weeks follow-up visit for all HHCs with negative IGRA results at the baseline evaluation, and participants were telephonically followed-up for 1 year to screen for symptoms of new active TB cases developing.

Participants were classified as: (a) “non-TBI” if the IGRA was negative both at baseline and at the 12-weeks evaluation, and they did not develop active TB on 1-year follow-up; (b) “pre-TBI” if the IGRA was negative at baseline evaluation but converted to positive IGRA at 12-weeks, or if the participant developed active TB on 1-year follow-up, and (c) “TBI” if the IGRA test was already positive at the baseline visit. Considering the known variability of the IGRA test around the positivity cut-off⁵⁷, we included in the TBI category only HHCs with a positive IGRA result at baseline with CD4 or CD4-CD8 tubes IFN- γ values well above the positivity cut-off (≥ 1.0 UI/ml). Individuals who did not complete follow-up or had lower positive IGRA results ($\leq 0.35 - 0.99$ UI/ml) were excluded from the analysis (Supplementary Fig. S1).

Ethical approval. The study has ethical approval from the Institutional Review Board of the Pontificia Universidad Católica de Chile. All eligible participants provided written informed consent. All methods were performed in accordance with the relevant guidelines and regulations.

Nasopharyngeal sample collection. Nasopharyngeal samples were collected with Flocked swabs (Copan®, California, United States). For 16S sequencing, samples were stored in 2 ml of DNA preservative solution tubes (Norgen Biotek Corp., Ontario, Canada), kept on ice and then stored within 1 to 4 h of collection at -80 °C until processing. Only one nasopharyngeal swab sample per participant—collected at the baseline visit—was analyzed. For Mtb culture, samples were stored in 2 ml PBS tubes and kept at room temperature until processing.

16S rRNA gene sequencing. Frozen swabs were thawed at room temperature and vortexed. Total DNA extraction of 500 μ l was performed using the Saliva DNA Isolation Kit (Norgen Biotek Corp., Ontario, Canada) according to the manufacturer's supplementary protocol instructions at Instituto de Ciencias Biomédicas, Universidad de Chile. Frozen samples were shipped and sequenced at the Genomics Center of the University of Minnesota (Minneapolis, United States). Briefly, the genomic DNA (gDNA) content was quantified via qPCR of the 16S rRNA gene and used to normalize the gDNA concentration samples before library preparation. Libraries were prepared by amplifying the V1-V3 region of the 16S rRNA gene with 25 PCR cycles using the Nextera sequencing kit (Illumina, California, United States). Sequencing was performed with MiSeq 600 cycle v3 kit.

Data processing and analysis. *Amplicon sequencing variant generation.* Sequencing data were processed with the DADA2 package⁵⁸ in R version 4.2.0⁵⁹ to generate amplicon sequencing variants (ASVs). Sequence quality was manually inspected to define trimming parameters. For sequence filtering and trimming, DADA2 function *filterAndTrim* was used with the following parameters: trimLeft = c(20,18), truncLen = c(290,275), maxEE = c(5,7), maxN = 0, truncq = 0. Error rates were estimated from the total dataset with the function *learnErrors* and the following parameters: max_consist = 20, nbases = 1e8. ASVs were generated with the *dada* function in pseudo-pooling mode. Read pairs were merged using the *mergePairs* function with minOverlap = 10 and maxMismatch = 1. Finally, the removal of chimeric sequences was done with the *removeBimeraDenovo* function using a consensus approach. The resulting ASVs were annotated using the *assignTaxonomy* function of DADA2 against the SILVA 138 database⁶⁰. A phylogenetic tree was constructed for all ASVs by aligning them using MAFFT version 7.475⁶¹ and FastTree version 2.1.10⁶² using a General Time Reversible (GTR) model.

ASV analysis. ASV filtering. ASVs were removed if present in two different set control (preservation buffer and two water controls) used for library construction before sequencing. After ASVs generation, samples with less than 1,000 reads were also removed in a second filtering stage, as well as any ASV within the dataset classified as either contaminant (*Chloroplast*, *Mitochondria* or *Eukaryota*) or taxa with low prevalence (1 ASV in 1 sample at the Phylum level – *Abditibacteriota*, *Campylobacterota*, *Cloacimonadota*, *Entotheonellaeota*, *Elusimicrobiota*, *Halanaerobiaeota*, *Hydrogenedentes*, *Methylomirabilota*, *Nitrospinota*, *Nitrospirota*, SAR324 clade, *Sumerlaeota*, *Synergistota*, WOR-1, WS2, and WPS-2), keeping only ASVs present in at least four samples (5% of the dataset).

Microbiome analysis, alpha and beta diversity. Composition analysis of the cleaned dataset (841 ASVs) was done using *phyloseq*⁶³ and its visualization with the *ggplot2* package⁶⁴. Core microbiome analysis was performed using the *microbiome* package⁶⁵. A core microbiome for each group (non-TBI, pre-TBI and TBI) was generated using a detection threshold of 0.001 and a prevalence of 50% of the samples within the group at the ASV and genus classification level.

For alpha diversity analysis, Shannon values were calculated using *phyloseq*⁶³ for each sample. A Kruskal–Wallis test followed by a Wilcoxon test with Holm adjustment for multiple testing was applied to assess pairwise differences. Analysis and visualization were performed using the *ggstatsplot* package⁶⁶.

Beta diversity was estimated using the compositional data (raw counts) and processed with the *PhILR* package⁶⁷ to normalize counts with an isometric log-ratio transformation using the phylogenetic tree information (distance of the ASVs present in the samples). Sample distance was calculated on the transformed dataset with Euclidean distance using the *phyloseq* package⁶³. To evaluate statistical differences between group clustering, a permutational analysis of variance was performed on the Euclidean distance matrix using the *adonis* function of the *vegan* package⁶⁸. The variance homogeneity assumption was evaluated using the functions *betadisperser* and *permutest* of the *vegan* package.

Differentially abundant taxa. The compositional approach implemented in ANCOMBC⁶⁹ that allows for compositional analysis of the microbiome data with bias correction was used to identify taxonomic groups with statistically significant differences in abundance between HHCs groups. This method acknowledges sources of variation in microbiome datasets, including unequal sampling fractions and differences in sequencing efficiency, to attempt to limit the effects of group unevenness due to the microbiome variability among individuals in our study. The ASVs were summarized at the genus level, and all three pairwise comparisons of the groups (non-TBI vs. TBI, non-TBI vs. pre-TBI, and pre-TBI vs. TBI) were performed using default parameters. Multiple hypothesis testing was corrected with the Benjamini–Hochberg method with a false discovery rate of 0.05; the resulting differentially abundant ASVs were filtered, keeping only those with a log fold change of at least 0.5.

Statistical analysis. Clinical and demographic data analyses were performed in RStudio^{59,70}. Comparisons between groups were performed with analysis of variance (ANOVA) for continuous variables, and Fisher's exact or Chi-squared test for categorical variables. Statistical significance was considered when p-values < 0.05 (two-tailed).

Data availability

The datasets generated and/or analyzed during the current study are available in the European Nucleotide Archive (ENA), Project Accession number PRJEB61078.

Received: 22 December 2022; Accepted: 24 April 2023

Published online: 05 May 2023

References

- Global tuberculosis report 2020. (Geneva: World Health Organization; 2020. Licence: CC BY-NC-SA 3.0 IGO).
- Acuña-Villaorduna, C. *et al.* Intensity of exposure to pulmonary tuberculosis determines risk of tuberculosis infection and disease. *Eur. Respir. J.* **51**, 1. <https://doi.org/10.1183/13993003.01578-2017> (2018).
- Reichler, M. R. *et al.* Duration of exposure among close contacts of patients with infectious tuberculosis and risk of latent tuberculosis infection. *Clin. Infect. Dis.* **71**, 1627–1634. <https://doi.org/10.1093/cid/ciz1044> (2020).
- Narasimhan, P., Wood, J., Macintyre, C. R. & Mathai, D. Risk factors for tuberculosis. *Pulm Med* **2013**, 828939. <https://doi.org/10.1155/2013/828939> (2013).
- Salgame, P., Geadas, C., Collins, L., Jones-Lopez, E. & Ellner, J. J. Latent tuberculosis infection—Revisiting and revising concepts. *Tuberculosis (Edinb.)* **95**, 373–384. <https://doi.org/10.1016/j.tube.2015.04.003> (2015).
- Casadevall, A. & Pirofski, L. A. What is a host? Incorporating the microbiota into the damage–response framework. *Infect. Immun.* **83**, 2–7. <https://doi.org/10.1128/IAI.02627-14> (2015).
- Young, V. B. The role of the microbiome in human health and disease: An introduction for clinicians. *BMJ* **356**, 831. <https://doi.org/10.1136/bmj.j831> (2017).
- Zhang, Y., Lun, C. Y. & Tsui, S. K. Metagenomics: A New Way to Illustrate the Crosstalk between Infectious Diseases and Host Microbiome. *Int. J. Mol. Sci.* **16**, 26263–26279. <https://doi.org/10.3390/ijms161125957> (2015).
- Waldman, A. J. & Balskus, E. P. The human microbiota, infectious disease, and global health: Challenges and opportunities. *ACS Infect. Dis.* **4**, 14–26. <https://doi.org/10.1021/acinfecdis.7b00232> (2018).
- Man, W. H., de SteenhuijsenPiters, W. A. & Bogaert, D. The microbiota of the respiratory tract: gatekeeper to respiratory health. *Nat. Rev. Microbiol.* **15**, 259–270. <https://doi.org/10.1038/nrmicro.2017.14> (2017).
- Ventero, M. P. *et al.* Nasopharyngeal Microbial Communities of Patients Infected With SARS-CoV-2 That Developed COVID-19. *Front. Microbiol.* **12**, 637430. <https://doi.org/10.3389/fmicb.2021.637430> (2021).
- Kang, H. M. & Kang, J. H. Effects of nasopharyngeal microbiota in respiratory infections and allergies. *Clin. Exp. Pediatr.* **64**, 543–551. <https://doi.org/10.3345/cep.2020.01452> (2021).
- Dai, W. *et al.* The concordance between upper and lower respiratory microbiota in children with Mycoplasma pneumoniae pneumonia. *Emerg. Microbes Infect.* **7**, 92. <https://doi.org/10.1038/s41426-018-0097-y> (2018).
- Sakwinska, O. *et al.* Nasopharyngeal microbiota in healthy children and pneumonia patients. *J. Clin. Microbiol.* **52**, 1590–1594. <https://doi.org/10.1128/JCM.03280-13> (2014).
- Haak, B. W. *et al.* Bacterial and viral respiratory tract microbiota and host characteristics in adults with lower respiratory tract infections: A case-control study. *Clin. Infect. Dis.* **74**, 776–784. <https://doi.org/10.1093/cid/ciab568> (2022).
- Creemers, A. J. *et al.* The adult nasopharyngeal microbiome as a determinant of pneumococcal acquisition. *Microbiome* **2**, 44. <https://doi.org/10.1186/2049-2618-2-44> (2014).
- Botero, L. E. *et al.* Respiratory tract clinical sample selection for microbiota analysis in patients with pulmonary tuberculosis. *Microbiome* **2**, 29. <https://doi.org/10.1186/2049-2618-2-29> (2014).
- Li, W., Zhu, Y., Liao, Q., Wang, Z. & Wan, C. Characterization of gut microbiota in children with pulmonary tuberculosis. *BMC Pediatr.* **19**, 445. <https://doi.org/10.1186/s12887-019-1782-2> (2019).
- Warndorff, D. K. *et al.* Polymerase chain reaction of nasal swabs from tuberculosis patients and their contacts. *Int. J. Leprosy* **64**, 404–408 (1996).
- Balcells, M. E. *et al.* M. tuberculosis DNA detection in nasopharyngeal mucosa can precede tuberculosis development in contacts. *Int. J. Tuberc. Lung Dis.* **20**, 848–852. <https://doi.org/10.5588/ijtld.15.0872> (2016).
- Budden, K. F. *et al.* Emerging pathogenic links between microbiota and the gut-lung axis. *Nat. Rev. Microbiol.* **15**, 55–63. <https://doi.org/10.1038/nrmicro.2016.142> (2017).
- Khan, N. *et al.* Alteration in the Gut Microbiota Provokes Susceptibility to Tuberculosis. *Front. Immunol.* **7**, 529. <https://doi.org/10.3389/fimmu.2016.00529> (2016).
- Perry, S. *et al.* Infection with Helicobacter pylori is associated with protection against tuberculosis. *PLoS One* **5**, e8804. <https://doi.org/10.1371/journal.pone.0008804> (2010).
- Wang, J. *et al.* Bacterial colonization dampens influenza-mediated acute lung injury via induction of M2 alveolar macrophages. *Nat. Commun.* **4**, 2106. <https://doi.org/10.1038/ncomms3106> (2013).
- Rice, T. A. *et al.* Signaling via pattern recognition receptors NOD2 and TLR2 contributes to immunomodulatory control of lethal pneumovirus infection. *Antiviral Res.* **132**, 131–140. <https://doi.org/10.1016/j.antiviral.2016.06.002> (2016).
- Qin, T. *et al.* Super-dominant pathobiontic bacteria in the nasopharyngeal microbiota as causative agents of secondary bacterial infection in influenza patients. *Emerg. Microbes Infect.* **9**, 605–615. <https://doi.org/10.1080/22221751.2020.1737578> (2020).
- Ling, Z. *et al.* Pyrosequencing analysis of the human microbiota of healthy Chinese undergraduates. *BMC Genom.* **14**, 390. <https://doi.org/10.1186/1471-2164-14-390> (2013).
- Nardelli, C. *et al.* Nasopharyngeal microbiome signature in COVID-19 positive patients: Can we definitively get a role to fusobacterium periodonticum?. *Front Cell Infect Microbiol* **11**, 625581. <https://doi.org/10.3389/fcimb.2021.625581> (2021).
- Edouard, S. *et al.* The nasopharyngeal microbiota in patients with viral respiratory tract infections is enriched in bacterial pathogens. *Eur J Clin Microbiol Infect Dis* **37**, 1725–1733. <https://doi.org/10.1007/s10096-018-3305-8> (2018).
- Rouchka, E. C. *et al.* Induction of interferon response by high viral loads at early stage infection may protect against severe outcomes in COVID-19 patients. *Sci. Rep.* **11**, 15715. <https://doi.org/10.1038/s41598-021-95197-y> (2021).
- Allen, E. K. *et al.* Characterization of the nasopharyngeal microbiota in health and during rhinovirus challenge. *Microbiome* **2**, 22. <https://doi.org/10.1186/2049-2618-2-22> (2014).
- De Boeck, I. *et al.* Comparing the healthy nose and nasopharynx microbiota reveals continuity as well as niche-specificity. *Front. Microbiol.* **8**, 2372. <https://doi.org/10.3389/fmicb.2017.02372> (2017).
- Huang, Y. *et al.* Alterations in the nasopharyngeal microbiota associated with active and latent tuberculosis. *Tuberculosis* <https://doi.org/10.1016/j.tube.2022.102231> (2022).
- Eribo, O. A. *et al.* The gut microbiome in tuberculosis susceptibility and treatment response: guilty or not guilty?. *Cell Mol. Life Sci.* **77**, 1497–1509. <https://doi.org/10.1007/s00018-019-03370-4> (2020).
- Naidoo, C. C. *et al.* The microbiome and tuberculosis: state of the art, potential applications, and defining the clinical research agenda. *Lancet Respir. Med.* **7**, 892–906. [https://doi.org/10.1016/s2213-2600\(18\)30501-0](https://doi.org/10.1016/s2213-2600(18)30501-0) (2019).
- Cheung, M. K. *et al.* Sputum microbiota in tuberculosis as revealed by 16S rRNA pyrosequencing. *PLoS One* **8**, e54574. doi:<https://doi.org/10.1371/journal.pone.0054574> (2013).
- Cui, Z. *et al.* Complex sputum microbial composition in patients with pulmonary tuberculosis. *BMC Microbiol.* **12**, 276. <https://doi.org/10.1186/1471-2180-12-276> (2012).
- Hong, B. Y., Paulson, J. N., Stine, O. C., Weinstock, G. M. & Cervantes, J. L. Meta-analysis of the lung microbiota in pulmonary tuberculosis. *Tuberculosis (Edinb.)* **109**, 102–108. <https://doi.org/10.1016/j.tube.2018.02.006> (2018).
- Hu, Y. *et al.* Metagenomic analysis of the lung microbiome in pulmonary tuberculosis—A pilot study. *Emerg. Microbes Infect.* **9**, 1444–1452. <https://doi.org/10.1080/22221751.2020.1783188> (2020).
- Wu, J. *et al.* Sputum microbiota associated with new, recurrent and treatment failure tuberculosis. *PLoS One* **8**, e83445. doi:<https://doi.org/10.1371/journal.pone.0083445> (2013).

41. Escapa, I. F. *et al.* New Insights into Human Nostril Microbiome from the Expanded Human Oral Microbiome Database (eHOMD): a Resource for the Microbiome of the Human Aerodigestive Tract. *mSystems* **3**, 1. <https://doi.org/10.1128/mSystems.00187-18> (2018).
42. Callahan, B. J., McMurdie, P. J. & Holmes, S. P. Exact sequence variants should replace operational taxonomic units in marker-gene data analysis. *ISME J.* **11**, 2639–2643. <https://doi.org/10.1038/ismej.2017.119> (2017).
43. De Boeck, I. *et al.* The nasal mutualist *Dolosigranulum pigrum* AMBR11 supports homeostasis via multiple mechanisms. *iScience* **24**, 1078. <https://doi.org/10.1016/j.isci.2021.102978> (2021).
44. Laufer, A. S. *et al.* Microbial communities of the upper respiratory tract and otitis media in children. *mBio* **2**, e00245–00210. <https://doi.org/10.1128/mBio.00245-10> (2011).
45. Pettigrew, M. M. *et al.* Upper respiratory tract microbial communities, acute otitis media pathogens, and antibiotic use in healthy and sick children. *Appl Environ Microbiol* **78**, 6262–6270. <https://doi.org/10.1128/AEM.01051-12> (2012).
46. Brugger, S. D. *et al.* *Dolosigranulum pigrum* cooperation and competition in human nasal microbiota. *mSphere* **5**, 1. <https://doi.org/10.1128/mSphere.00852-20> (2020).
47. Laclaire, L. & Facklam, R. Antimicrobial susceptibility and clinical sources of *Dolosigranulum pigrum* cultures. *Antimicrob Agents Chemother* **44**, 2001–2003. <https://doi.org/10.1128/AAC.44.7.2001-2003.2000> (2000).
48. Rueda, M. *et al.* Investigation of nasal/oropharyngeal microbial community of COVID-19 patients by 16S rDNA sequencing. *Int. J. Environ. Res. Public Health* **18**, 1. <https://doi.org/10.3390/ijerph18042174> (2021).
49. Jamieson, W. D., Pehl, M. J., Gregory, G. A. & Orwin, P. M. Coordinated surface activities in *Variovorax paradoxus* EPS. *BMC Microbiol* **9**, 124. <https://doi.org/10.1186/1471-2180-9-124> (2009).
50. Mindt, B. C. & DiGiandomenico, A. Microbiome Modulation as a Novel Strategy to Treat and Prevent Respiratory Infections. *Antibiotics (Basel)* **11**, 1. <https://doi.org/10.3390/antibiotics11040474> (2022).
51. Ma, S. *et al.* Metagenomic analysis reveals oropharyngeal microbiota alterations in patients with COVID-19. *Signal Transduct. Target Ther.* **6**, 191. <https://doi.org/10.1038/s41392-021-00614-3> (2021).
52. Bayal, N. *et al.* Structural aspects of lesional and non-lesional skin microbiota reveal key community changes in leprosy patients from India. *Sci. Rep.* **11**, 3294. <https://doi.org/10.1038/s41598-020-80533-5> (2021).
53. van Rensburg, J. J. *et al.* The Human Skin Microbiome Associates with the Outcome of and Is Influenced by Bacterial Infection. *mBio* **6**, e01315–01315. doi:<https://doi.org/10.1128/mBio.01315-15> (2015).
54. Kumpitsch, C., Koskinen, K., Schopf, V. & Moissl-Eichinger, C. The microbiome of the upper respiratory tract in health and disease. *BMC Biol.* **17**, 87. <https://doi.org/10.1186/s12915-019-0703-z> (2019).
55. Wilmski, T. *et al.* Gut microbiome pattern reflects healthy ageing and predicts survival in humans. *Nat. Metab.* **3**, 274–286. <https://doi.org/10.1038/s42255-021-00348-0> (2021).
56. Balcells, M. E. *et al.* Systematic screening of adult household contacts of patients with active pulmonary tuberculosis reveals high rates of new infections during follow-up. *Rev. Med. Chil.* **148**, 151–159. <https://doi.org/10.4067/s0034-98872020000200151> (2020).
57. Wikell, A. *et al.* The Impact of Borderline Quantiferon-TB Gold Plus Results for Latent Tuberculosis Screening under Routine Conditions in a Low-Endemicity Setting. *J. Clin. Microbiol.* **59**, e0137021. <https://doi.org/10.1128/JCM.01370-21> (2021).
58. Callahan, B. J. *et al.* DADA2: High-resolution sample inference from Illumina amplicon data. *Nat. Methods* **13**, 581–583. <https://doi.org/10.1038/nmeth.3869> (2016).
59. R: A language and environment for statistical computing. <https://www.R-project.org/> (2021).
60. Quast, C. *et al.* The SILVA ribosomal RNA gene database project: Improved data processing and web-based tools. *Nucl. Acids Res.* **41**, D590–596. <https://doi.org/10.1093/nar/gks1219> (2013).
61. Katoh, K. & Standley, D. M. MAFFT multiple sequence alignment software version 7: Improvements in performance and usability. *Mol. Biol. Evol.* **30**, 772–780. <https://doi.org/10.1093/molbev/mst010> (2013).
62. Price, M. N., Dehal, P. S. & Arkin, A. P. FastTree 2--approximately maximum-likelihood trees for large alignments. *PLoS One* **5**, e9490. <https://doi.org/10.1371/journal.pone.0009490> (2010).
63. McMurdie, P. J. & Holmes, S. phyloseq: an R package for reproducible interactive analysis and graphics of microbiome census data. *PLoS One* **8**, e61217. <https://doi.org/10.1371/journal.pone.0061217> (2013).
64. Wickham, H. *ggplot2*. (Springer Science+Business Media, 2009).
65. Lahti, L. & Shetty, S. *Tools for microbiome analysis in R*. <http://microbiome.github.com/microbiome> (2017).
66. Patil, I. Visualizations with statistical details: The 'ggstatsplot' approach. *J. Open Source Softw.* **6**, <https://doi.org/10.21105/joss.03167> (2021).
67. Silverman, J. D., Washburne, A. D., Mukherjee, S. & David, L. A. A phylogenetic transform enhances analysis of compositional microbiota data. *Elife* **6**, doi:<https://doi.org/10.7554/eLife.21887> (2017).
68. Oksanen, J. *et al.* (2020). vegan: Community Ecology Package. R package version 2.5–7. <https://CRAN.R-project.org/package=vegan>.
69. Lin, H. & Peddada, S. D. Analysis of compositions of microbiomes with bias correction. *Nat Commun* **11**, 3514. <https://doi.org/10.1038/s41467-020-17041-7> (2020).
70. RStudio: Integrated Development for R. RStudio, PBC. <http://www.rstudio.com/>. (2020).

Acknowledgements

This work was supported by ANID/CONICYT FONDECYT [1171570 and 1211225 to M.E.B, 1191874 to R.N, 11140666 and 1221209 to J.A.U.].

Author contributions

M.E.B. and R.N. worked in the conception and design of the work, C.R.-T. and M.E.B. wrote the main manuscript text, J.A.U. made the microbiome statistical analyses and prepared the figures, C.R.-T. made clinical and demographic statistical analyses and prepared the tables. All authors reviewed the manuscript.

Competing interests

The authors declare no competing interests.

Additional information

Supplementary Information The online version contains supplementary material available at <https://doi.org/10.1038/s41598-023-34052-8>.

Correspondence and requests for materials should be addressed to M.E.B.

Reprints and permissions information is available at www.nature.com/reprints.

Publisher's note Springer Nature remains neutral with regard to jurisdictional claims in published maps and institutional affiliations.



Open Access This article is licensed under a Creative Commons Attribution 4.0 International License, which permits use, sharing, adaptation, distribution and reproduction in any medium or format, as long as you give appropriate credit to the original author(s) and the source, provide a link to the Creative Commons licence, and indicate if changes were made. The images or other third party material in this article are included in the article's Creative Commons licence, unless indicated otherwise in a credit line to the material. If material is not included in the article's Creative Commons licence and your intended use is not permitted by statutory regulation or exceeds the permitted use, you will need to obtain permission directly from the copyright holder. To view a copy of this licence, visit <http://creativecommons.org/licenses/by/4.0/>.

© The Author(s) 2023